Macromolecules **2007,** *40,* 7771−7776

Sequence Positioning of Disulfide Linkages to Program the Degradation of Monodisperse Poly(amidoamines)

Laura Hartmann,[†] Stefanie Häfele,[‡] Regine Peschka-Süss,[‡] Markus Antonietti,[†] and Hans G. Börner*,[†]

Department of Colloids, Max Planck Institute of Colloids and Interfaces, Am Muehlenberg 1, D-14476 Golm, Germany, and Department of Pharmaceutical Technology and Biopharmacy, Albert-Ludwigs-University, Stefan-Meier-Strasse 19, D-79104 Freiburg, Germany

Received June 27, 2007; Revised Manuscript Received August 14, 2007

ABSTRACT: A polymer drug-carrier was synthesized by combining a monodisperse, sequence-defined poly(amidoamine) segment with a poly(ethylene oxide)-block (PAA-*block*-PEO). Between both polymer blocks a single disulfide moiety is incorporated that allows for the realization of a programmed disassembly of the carrier polymer in a reductive environment, like for instance present in certain intracellular compartments. The sequence selective positioning is realized using cystamine as a new building block for the automated synthesis of monodisperse PAAs. The controlled disassembly of the polymeric carrier was used to establish a two-phase release process, e.g., highly relevant for an effective release after successful drug delivery into a cell. The applicability of this carrier was demonstrated by analyzing the complexation behavior of the system with plasmid DNA, before and after reductive degradation of the block copolymer. The presented observations describe a transition in polyplex (polymer−DNA complex) properties from PEO-stabilized ion complexes with soft charge compensation to compact structures with more effective charge neutralization after cleavage of the PEO-block.

Introduction

Recently, linear poly(amidoamine)s (PAA)s have been recognized as a class of (multi)functional polymers, highly interesting for a broad scope of different biomedical applications.[1,2] Their potential was revealed by proving excellent biocompatibility, usually combined with the absence of inherent immunogenicity as well as very low cyto- and hemotoxicity.[3−7] Despite all these advantages, the full potentials of this promising polymers could still not be accessed. This is due to the applied synthesis strategies, following Michael-addition routes, which provide polydisperse polymers with $M_w/M_n \geq 2$.[8,9]

To overcome these synthetic obstacles, a more precise approach to linear PAAs was presented recently.[10] This involved fully automated, solid-phase supported synthesis techniques, combined with protecting group strategies, which allowed for the sequential addition of monomers. Monodisperse PAAs with monomer sequence control could be accessed, thus making the precise positioning of different functionalities along the PAA chain possible. Because the PAA synthesis still remains compatible to the synthesis of peptides, it was possible to fully automate the PAA synthesis, including the change of the “monomer alphabets” to obtain peptide-*block*-PAA and PEO-*block*-PAA conjugates in a straightforward manner.[11]

Polymers used as drug delivery applications have to provide stability and shielding of the cargo during the transport, but effective and controlled liberation of the drug at the appropriate destination. Moreover, because the control of the fate of carrier polymers in the living system is a growing issue, a final degradation of the polymer systems to nontoxic fragments that are rapidly cleared from the organism is certainly favorable. Hence, the precise positioning of specific functions is mandatory to design suitable polymer systems, which meet the requirements of both advanced drug delivery systems and legislation for product registration.

Controlled degradation of polymer carriers has been addressed in the literature intensively. Frequently degradable polymer carriers, like, for instance, polyesters, decompose via hydrolytic or enzymatic pathways.[12,13] These can be amplified by the localization of the carrier in a certain cell compartment, e.g., in the lysosome.

Recently, the introduction of disulfide linkages within the polymer backbone of carriers received increased attention as an alternative to hydrolytically degradable systems. Disulfide bonds are stable in the oxidative environment of extracellular fluids but are rapidly degraded intracellularly, due to the reductive environment caused by an increased concentration of glutathione.[14] These specific properties have been exploited to develop polymers, which undergo a controlled degradation after uptake into a cell, e.g., triggering then the drug release. Several polymers for biomedical applications, bearing such disulfide functionalities along the polymer chain, were described, e.g., poly(ethylenimine)s, poly(ethylene oxide)s and linear PAAs.[15−17] However, so far introduction of the disulfide functionalities was accomplished either in a statistical or in an alternating manner. Here, we want to extend this approach to a precisely programmed disassembly, in order to realize precisely defined functions. For that, the exact positioning of cleavable groups in the polymer chain is required, enabling the rational design of polymeric drug carriers with advanced functions beyond those of established carrier systems.

Particularly the demands concerning polymers, which should be utilized as polymeric vectors for in vivo DNA delivery are rather complex.[18] This is due to the fact that the delivery process requires the transition of multiple barriers and the trafficking of the cargo into the cell nucleus, the most protected cell compartment. The schematic multistep pathway, required to deliver DNA into the nucleus, is illustrated in Figure 1. Here it

---

* Corresponding author. E-mail: Hans.boerner@mpikg.mpg.de. Telephone: +49 (0)331-567-9552. Fax: +49 (0)331-567-9502.

[†] Department of Colloids, Max Planck Institute of Colloids and Interfaces.

[‡] Department of Pharmaceutical Technology and Biopharmacy, Albert-Ludwigs-University.

10.1021/ma071427u CCC: \$37.00

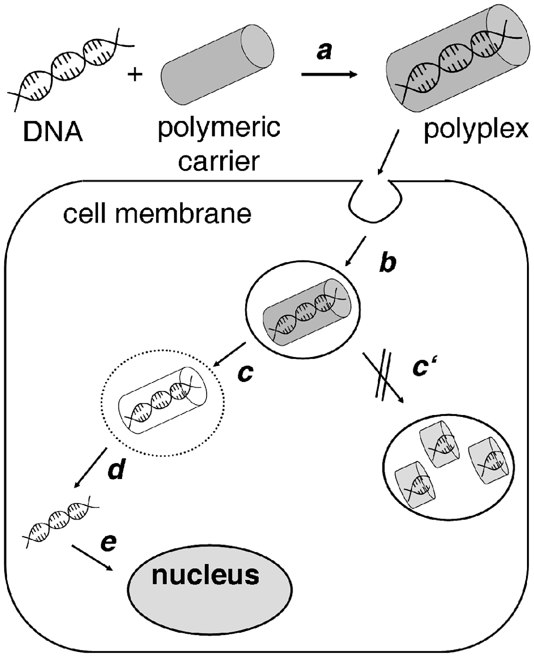

Figure 1. Simplified model for polymer facilitated delivery of DNA (transfection mechanism): complex formation of the cationic carrier and the anionic DNA (polyplex formation, a); internalization of the polyplex into an endosome (membrane translocation, b); release of the polyplex from the endosome (endosomal escape, c) or delivery of the polyplex into the lysosome and enzymatic degradation (c′); liberation of the DNA from the polymeric carrier (d); localization of the DNA in the cell nucleus (e).

should be noted that the precise mechanism is still not understood, and hence, the presented scheme has to be regarded as highly simplified.

The first step toward successful DNA delivery is the effective complexation of the negatively charged plasmid *double strand* DNA (*ds*DNA) with a cationic polymer carrier (Figure 1a). The formed polyplex (polymer−DNA ion complex) is incorporated into a cell by crossing the cell membrane (Figure 1b). Several different uptake pathways are known, but still heavily discussed.[19] However, the successful internalization of the polyplex leads—in the simplest case—to an incorporation encapsulation into an intracellular compartment, which is referred to as an endosome (Figure 1b). Typically the endosome is transformed into the lysosome, a compartment where enzymatic digestion would destroy the DNA (Figure 1c′). Therefore, the polyplex has to escape from the endosome, prior to reaching the lysosome (Figure 1c). This crucial endosomal escape can be facilitated by the properties of the polymeric carrier, leading to interesting strategies in the design of polymer carriers.[21−23] Some of the strategies include the liberation of the DNA from the polyplex, e.g., by degradation of the carriers via pH-cleavable groups in the polymer chain (Figure 1d). In the last step the DNA has to be translocated into the cell nucleus (Figure 1e). For that a crossing of the core membrane is required. Even if the process of nucleus localization is not understood yet, it appears to be reasonable that nuclear membrane crossing could be affected by the carrier polymer, too.

Here we demonstrate first steps toward a multistep release carrier for DNA-delivery, exploiting programmable disassembly of the polymeric carrier. The function was realized by the sequence selective positioning of a disulfide functionality within a PEO-*block*-PAA system. For that cystamine (2,2′-dithiobis-(ethylamine)) was utilized as a new building block for the automated synthesis of monodisperse PAA segments enabling the predetermination of the splitting point. The applicability of this polymer as carrier system for DNA delivery was investigated by analyzing the structure of the complex of carrier polymer with plasmid *ds*DNA, before and after reductive disassembly.

Experimental Section

Materials and Instrumentation. See Supporting Information.

General Synthesis of Poly(amidoamine) (PAA) Conjugates. The monodisperse, sequence-defined PAA segments were prepared via a solid-phase supported synthesis as was reported previously.[10] As for the classical solid-phase peptide synthesis (SPPS) based on Merrifield, using the stepwise addition of amino acids, the PAAs segments are synthesized by a stepwise assembly of dicarboxylate and diamine building blocks. In a first step, a dicarboxylate building block, activated as succinic anhydride (Suc), was coupled to a resin bound amino group. High conversion was controlled via colorimetric tests and mass spectrometry, also indicating no side reactions. The subsequent coupling of a diamine building block was enabled using PyBOP/HOBt/DIPEA, a frequent activating reagent for carboxylate functionalities in SPPS. Again, high conversion was secured via colorimetric tests and mass spectrometry. The repetitive coupling of dicarboxylate and diamine building blocks following these standard protocols leads to PAA segments of up to 10 repeating units. To vary the functionalities within the PAA sequence, different diamine building blocks can be used. For the introduction of tertiary amine groups 3,3′-diamino-*N*-methyldipropylamine (Damp) was used. For the incorporation of secondary amine groups a spermine (Spe) derivative was synthesized bearing *t*Boc protective groups at the secondary amine functionalities. By driving each step to completion, a monodisperse system is obtained, offering a monomer sequence along the polymer backbone that depends on the choice of building blocks at every single addition. Side groups of the building blocks have to be protected during the addition to avoid side reactions. The product can be liberated and the side-chain protecting groups can be cleaved in a one-step reaction, using TFA in DCM. The established PAA synthesis is fully compatible with standard peptide synthesis techniques. Therefore, amino acids or peptide sequences can be incorporated, e.g., to introduce primary amine functionalities using Lysin (Lys) as a building-block. Following established routes toward PEO-peptide conjugates, PEO−PAA conjugates can be obtained using PEO attached (PAP) resins.

Synthesis of PAA Segments Containing a Disulfide Linkage. To incorporate a disulfide linkage within the polymer backbone, a diamine building block containing a disulfide functionality, cystamine, was used. Cystamine (Cya) is only commercially available as hydrochloride salt, but for an addition to the activated carboxylate group the free diamine is needed. To isolate the free diamine, a solution of cystamine salt in water was made strongly basic by addition of sodium hydroxide solution and then extracted with chloroform, giving the product **I** as yellow oil (55%).

Analysis of **I**: ^{1}H NMR (DMSO, 100 °C) $\delta = 1.71$ (s, 4H, NH_2), 2.70 (t, 4H, CH_2−NH$_2$), 2.77 (t, 4H, S−CH_2) ppm; ^{13}C NMR (DMSO, 100 °C) $\delta = 40.0$ (s, CH$_2$−NH$_2$), 42.0 (s, S−CH$_2$); ESI-MS $m/z = 153$ ([M + H]$^+$).

This building block can be used, following the standard protocols for the automated synthesis of PAA segments.

Synthesis of PAA Segments Containing Amino Acids. Since the established synthesis is fully compatible with the standard peptide synthesis protocols, amino acids or peptide segments can be incorporated within the polymer backbone. Amino acids are used as their N_α-Fmoc-protected derivatives, which are coupled to the growing chain by activation of their carboxylate functionality and addition to the terminal amino group of the resin-bound polymer. For a standard synthesis (0.25 mmol, 1 equiv) a 10-fold excess of amino acid (2.5 mmol, 10 equiv) is dissolved in DMF (2.5 g) and activated with HBTU in DMF (0.37 g, 9.8 equiv, 0.17 g/L). After transferring the activated amino acid to the resin, the reaction vessel is agitated for 25 min. After intensive washing with DMF, the terminal Fmoc protecting group is cleaved by adding a solution of piperidine in DMF (20 vol. %). By detecting the UV-signal of the cleaved Fmoc group the conversion of the reaction can be determined. After washing the resin with DMF, the Fmoc-cleavage can be repeated to verify for the completeness of the reaction. As a next step either another amino acid or a dicarboxylate building block can be added to the terminal amino group of the resin-bound PAA chain. For the synthesis of PEO-*block*-Lys-(Suc-Cya-Lys_2)-(Suc-Damp-Lys_2)$_4$ (**V**) a Wang PAP resin was used as the solid support. The synthesis followed the general procedure described above. The polymer was cleaved from the solid support using TFA in DCM (30%). After evaporation of the solvent, the polymer was reprecipitated from MeOH/ether, dialyzed against water (MWCO: 3500) and freeze-dried to give the product as a colorless powder (31%). **V** is soluble in water apparently independent of the pH value (pH = 1−12). Moreover, it possesses excellent solubility in a broad range of organic solvents such as methanol, NMP, DMF, and THF, but it precipitates in dichloromethane or diethyl ether.

Analysis of **V**: ^{1}H NMR (DMSO, 100 °C) $\delta = 1.23-1.41$ (m, 22 H, β-CH_2−lysine), 1.49−1.63 (m, 22 H, γ-CH_2−lysine), 1.67−1.80 (m, 22 H, α-CH_2−lysine), 2.34−2.43 (m, 22 H, β-CH_2−amine), 2.71−2.85 (m, 34 H, δ-CH_2−lysine, α-CH_3−amine), 3.21−3.30 (m, 31 H, α-CH_2−amid), 3.33−3.75 (m, 280 H, O═C−CH_2−CH_2, O═C-(NH), O−CH_2−CH_2−PEO) ppm; MALDI−TOF $m/z = 5921.98$ ($[M + K]^+$), M_{th} = PEO_{75}-*block*-Lys-(Suc-Cya-Lys_2)-(Suc-Damp-Lys_2)$_4$; FT-IR (ν in cm^{-1}) 1645 (amid I), 1537 (amid II), 1145 (amine), 1199 (ether).

Cleavage from the Resin. The dried resin bearing the block copolymer **II** (0,05 mmol, 1 equiv) was swollen in freshly distilled and degassed DMF and a mixture of DTT (19 mg, 0.125 mmol, 2,5 equiv) in DMF was added. After this mixture was stirred under argon for 1 h, the resin was removed by filtration. By now the PAA segment with a free thiol end group **IIIb** was dissolved in the solution, while the PEO-block with a free thiol end group **IIIa** remained bound to the resin. To avoid uncontrolled reoxidation of the thiols, the PAA-segment as well as the PEO-block was oxidized in the presence of an excess of 2-mercaptoethanol. Therefore, a mixture of 2-mercaptoethanol (35 μL, 0,5 mmol, 10 equiv) in DMF was added to the solution of the DTT-cleavage as well as to the thoroughly washed resin (70 μL, 1 mmol, 20 equiv). By dropwise addition of iodine in DMF, the oxidation was driven to completeness indicated by a constant color change of the solutions to dark orange. The solution of the PAA-segment was then concentrated in high vacuum to remove the solvent. The residue was redissolved in water, dialyzed against water (MWCO: 500) and freeze-dried to give the colorless product **IVb**.

After washing the resin thoroughly with DMF and DCM, the PEO-block was cleaved from the solid support, following standard protocols with a solution of 5 vol. % TFA in DCM for 30 min. After evaporation of the solvent, the residue was reprecipitated from MeOH/ether giving a colorless product **IVa**.

Scheme 1. Reductive Cleavage of the PAA-Segment from a Resin-Bound PEO-*block*-PAA Copolymer and Subsequent Oxidative Capping with 2-Mercaptoethanol To Stabilize the Thiol-Functionalized Products

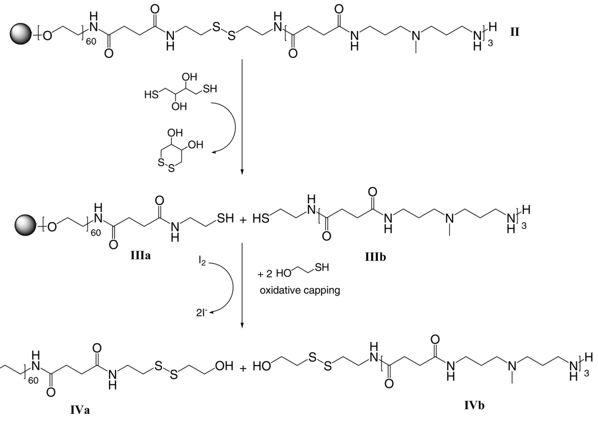

Results and Discussion

The main objective of this work was the introduction of precisely positioned disulfide functionalities within a monodispers PAA-segment. For that a solid-phase supported PAA synthesis route was applied as described previously.[10] Stepwise assembly of functional diamine and dicarboxylate building blocks, using a forced step-growth process, requires the control over every reaction step, driving monomer addition to quantitative conversion and suppressing side reactions. To realize this, highly optimized activation chemistry was adapted to meet the requirements of the PAA synthesis. Thus, the route allows for the synthesis of monodisperse PAAs, exhibiting a precisely defined monomer sequence and the absence of both chemical as well as molecular weight distributions.[10] In order to obtain a PEO-*block*-PAA block copolymer, a PEO preloaded polystyrene resin (PAP-resin) was used as solid support. While the PEO-block was attached to the PS support via a benzyl−ether-linker, a ω-amino functionality of the PEO can be used to sequentially assemble the PAA chain (PS−[benzyl]−O−PEO−NH_2). Since the linker connects the PEO and the PS-resin, a cleavage results in the liberation of the PEO-*block*-PAA copolymer.[11] As described previously, succinic acid anhydride was utilized as a pre-activated dicarboxylic acid building block, allowing a quantitative and clean attachment to the amine functionality of the resin. This generates resin-bound carboxylic acid functionalities to which a diamine building block can be coupled. The latter is facilitated by PyBOP/HOBt,[24] proceeds in a clean manner with quantitative conversion and generates a resin-bound amino group. The repetitive coupling of dicarboxylic acids and diamines leads to the sequential assembly of the linear PAA segment.

A model polymer (Scheme 1, **II**) was synthesized, in order to demonstrate the applicability of cystamine as a new diamine building block in the automated PAA synthesis. As shown in Scheme 1, cystamine was used to position a disulfide moiety between the blocks of a PEO-*block*-PAA copolymer. For ease of analysis, a short PAA segment was synthesized first that possesses three recurrences of alternating succinic anhydride (Suc) and 3,3′-diamino-*N*-methyldipropylamine (Damp). However, after the first Suc the cystamine was introduced, predetermining the position where reductive cleavage will take place.

To avoid difficulties during analysis, which might result from the superimposition of the PEO and the PAA-segment, the model cleavage of the disulfide bond was performed with DTT on a resin-bound PEO-*block*-PAA (Scheme 1). Reductive

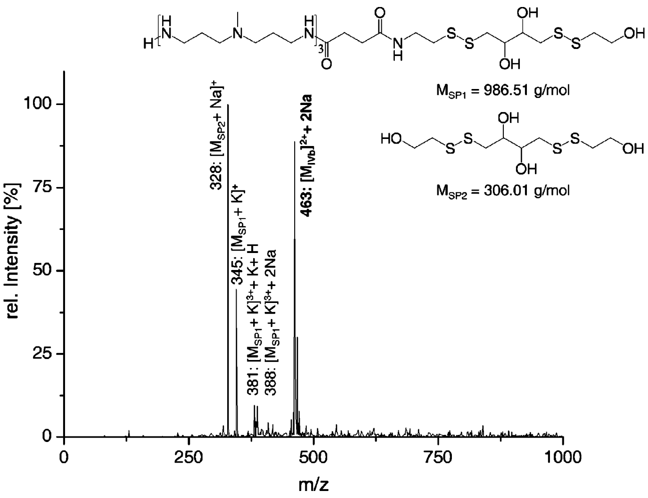

Figure 2. ESI mass spectrometry of the PAA segment (**IVb**) cleaved by reduction of the disulfide bond with DTT and oxidative capping with 2-mercaptoethanol.

cleavage results in the liberation of a PAA-segment with only tertiary amine groups. This can easily be detected by ESI−MS measurements, while the PEO-block remains bound to the solid-support. However, PEO and PAA segments are formed, exhibiting free thiol end groups. Because of a high sensitivity for uncontrolled oxidation or coupling, a controlled oxidation in the presence of high excess of 2-mercaptoethanol was carried out, leading to an oxidative capping (Scheme 1). The isolated PAA-segment was analyzed by ESI−MS (Figure 2), revealing both the successful synthesis of the monodisperse PAA segment and the clean cleavage of the disulfide bond. The ESI−MS shows the characteristic mass signal of **IVb** (*m*/*z* 462), which could be assigned within ±1 *m*/*z* accuracy to a double charged species with two sodium adduct ions ($M_{\mathbf{IVb,th.}} = 834$ Da).

Additional mass signals could be observed, corresponding conclusively to the product of the oxidative capping reaction as a result of the reaction of the DTT excess with 2-mercaptoethanol.

The capped PEO-block (**IVa**) was analyzed separately by MALDI−TOF MS (cf. Supporting Information). The spectrum shows two distributions centered at *m*/*z* 2615 and at *m*/*z* 3227 that can be assigned to mass signals of the PEO-block capped with 2-mercaptoethanol and those of the non-capped PEO-block (**IIIa**). The characteristic signal spacing of 44 *m*/*z* for both distributions can be correlated to the mass of a PEO repeat unit. Even though a complete capping reaction at the solid support was not possible, the cleavage of the disulfide bond is quantitative, because a distribution corresponding to the PEO−PAA precursor was not observed.

The independent characterization of the complete PEO-*block*-PAA (**II**) confirmed the chemical structure of the polymer, by showing a single distribution centered at *m*/*z* 3977. This could be assigned to the protonated product ion (cf. Supporting Information).

The sequence selective introduction of a disulfide moiety within the PAA backbone provides the possibility to generate specific activity profiles of the polymer carrier. Particularly this is interesting for polymeric carriers that should be applied for DNA-delivery. As discussed above the transport of DNA requires substantially different properties of the polyplex, depending on the delivery phase. While on the one hand PEO-shielding and soft cationic surface charges are of advantage, guaranteeing a safe transport of the polyplex to the cell, on the other hand small and cationic segments with effective charges but without PEO are needed to enhance endosomal escape and nuclear uptake. The latter is evident because certain oligopeptide domains like for instance TAT or Arg$_{10}$ have been recognized to enhance the membrane translocation.[21,25] Moreover, cells use small, cationic molecules such as spermine or spermidine to bind to DNA or RNA and control nuclear uptake.[26]

Translating this insight into a strategy, a polymeric carrier is required that allows for a two-step release of the DNA. This should (i) guarantee a safe transport of the DNA to the cell, (ii) facilitate endosomal escape of the cargo, and (iii) enhance transport of the DNA into the nucleus. For that a PEO-*block*-PAA conjugate was synthesized, bearing a single disulfide functionality between the two blocks. While the cationic PAA-segment is designed to complex and condense the plasmid *ds*DNA, the PEO-block shields the cargo effectively during transport and minimizes toxic side effects. After the successful cell internalization of the polyplex, the disulfide functionality should be cleaved. This leads to the removal of the protecting PEO-shell and boosts the efficiency of the PAA-segment for endosomal escape.[20] This is probably due to their cationic character combined with a weak amphiphilicity that allows for soft cell membrane interactions. Hence the intracellular generation of a “naked”, low molecular weight cationic PAA-segment should strongly enhance membrane interactions, which potentially could contribute to the endosomal escape and nucleus localization of the DNA cargo.

It is well-known that oligoamines with 3−4 cationic charges interact with DNA in a very dynamic manner.[27] Spermine leads, for example, to a more or less transient ion complex in which the oligocation can be displaced easily via competitive substitution. Taking this into account the PAA-segment of the model system (**II**) will not lead to sufficiently stable polyplexes with plasmid *ds*DNA. Thus, the synthesis of a PAA-segment with five recurrences of (lysine)−(lysine)−(diamino-*N*-methyldipropylamine)−(succinic acid) was required, bearing a sequence of tertiary and primary amines (**V**). This should guarantee strong interactions with the DNA, but also provide capabilities to interact with membranes for cation induced membrane bending. The successful synthesis of **V** was verified by means of MALDI−TOF mass spectrometry and ^{1}H NMR spectroscopy (cf. Supporting Information).

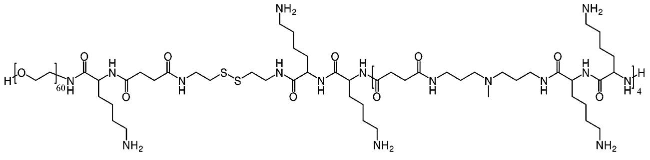

PEO$_{60}$-Lys-(Suc-**Cya**-Lys$_2$)-(Suc-Damp-Lys$_2$)$_4$ (**V**)

To investigate the complexation properties of the PEO-*block*-PAA copolymer **V** with plasmid DNA, both compounds were mixed at a *N*/*P* ratio of 10/1. The structure of the resulting polyplexes could be visualized by atomic force microscopy (AFM). Figure 3a shows the micrograph of the polyplexes, suggesting the formation of compact mono-plasmid polyplexes with coil-like structures. The radius of gyration of the polyplexes in solution as measured by light scattering was determined as 160 nm and corresponds well to the structures observed by AFM. It is likely that a positive net charge of the polyplexes can be assumed, because the structures absorb on the negatively charged mica substrate. Nevertheless the measured ζ potential of the polyplexes in buffered solution is practically zero. This is expected, due to steric shielding effects of the PEO-shell, shifting the hydrodynamic sliding plane of electrophoresis far

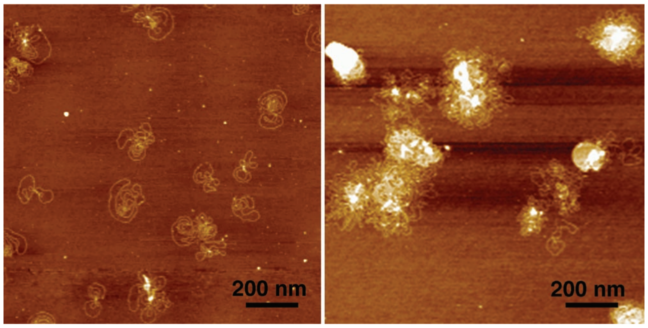

Figure 3. AFM micrographs of the polyplexes formed from PEO$_{60}$-Lys-(Suc-Cya-Lys$_2$)-(Suc-Damp-Lys$_2$)$_4$ (**V**) and plasmid *ds*DNA before (a, left) and after treatment with the reductive agent DTT (b, right) (*N*/*P* ratio 10/1, mica, phase-mode).

into the electrically neutral zone of the structures. This "hidden" cationic character might have additional advantages because nonspecific interactions with proteins are prevented, leading to a "stealth behavior". In contrast to polyplexes where branched poly(ethylenimine)s are used as carriers, the copolymer **V** apparently leads to soft and screened cationic charges, which is considered to be more compatible with biological systems. However, the polyplex is dynamic enough to interact with negatively charged surfaces, reflecting the possibility for membrane interactions.

Severe structural changes occur in the polyplexes after the disulfide linker between the PAA and the PEO-block was cleaved. To imitate the reductive cleavage that should take place intracellular after the uptake of the polyplex into a cell, DTT was added instead of glutathione due to ease of handling.

The addition of DTT to the polyplexes leads to a decrease of the radius of gyration, as evident from light scattering experiments in solution. The reduction from $R_g \sim 160$ nm for the untreated polyplexes to $R_g \sim 70$ nm of the reduced polyplexes could be explained as a result of the cleaved PEO-block. Probably this enables the ion complexes to adapt a denser electrostatic complexation and plasmid packing. Moreover, these experiments indicate that the aggregation tendency of the reduced polyplexes is not dramatically increased after removing the stabilizing PEO-shell. This could be interpreted as a first indication for a transition from steric to electrostatic stabilization, due to more effective cationic excess charges. These light scattering results are consistent with the AFM micrograph obtained from the solution of reduced polyplexes. As evidenced in Figure 3b, the detachment of the PEO-block by reductive means does not change the structure of the single polyplexes dramatically, but certainly gives a more dense packing motif. It should be noted that the tendency of the reduced polyplexes to form larger "clusters" on the mica substrate is presumably a methodic artifact due to wetting effects resulting in stronger adsorption in combination with higher local concentrations.

For further investigation of the property changes that result by cleaving the PEO segment from the polyplexes, gel electrophoresis experiments were performed, using agarose gels of the untreated as well as the reduced polyplexes (Figure 4).

Gel electrophoresis reveals the formation of stable polyplexes from a ratio of $N/P \geq 15/1$ as indicated by the retardation of the sample band (Figure 4). This retardation is usually interpreted as the increasing mass of the polyplex, resulting from the amount of polymer bound to the DNA, together with a reduction of the net charge of the complex. For the polyplexes formed at N/P ratios $\leq 15/1$ the negative charge of the DNA strand is not fully compensated by the polycation and therefore the sample band migrates toward the positive anode.

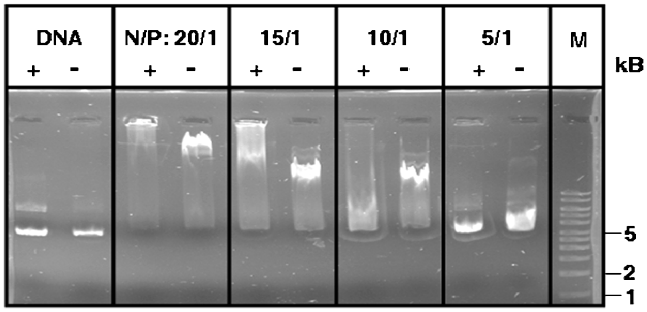

Figure 4. Gel electrophoresis of polyplexes formed with PEO-*block*-PAA copolymer **V** at different *N*/*P* ratios with (+) and without (−) the addition of the reductive agent DTT (M, standard DNA ladder indicating size in kilo bases (kB); separation direction, negative (top) to positive (bottom)).

The DTT cleavage of the PEO-block of polyplexes with a *N*/*P* ratio of 10/1 leads to a shift of the sample band to smaller molecular weights (Figure 4). This is consistent with the loss of the PEO-shell, which contributes ~51 wt % of the used PEO−PAA block copolymer. Increasing the *N*/*P* ratio to ≥ 15/1, a strong additional retardation of the sample band is observed after reduction. Taking into account that the light scattering experiments revealed the absence of aggregate formation, the strong retardation can be attributed to a more effective shielding of the negative charge of the DNA strand by complexation with the bare polycation. The absence of the shielding and sterically demanding PEO-blocks obviously enables an electrostatic rearrangement of the polyplex structure, resulting in a strong retardation of the sample band.

The presented electrophoresis data therefore strongly support the view of a switchable transition in polyplex properties from the original PEO-stabilized ion complexes with soft charge compensation to more compact structures with more effective charge neutralization. This transition could be triggered by the cleavage of the disulfide bond located between the PEO and the monodisperse PAA-segment in a PEO-*block*-PAA carrier.

Conclusions

Cystamine was presented as a convenient building block for the solid-phase supported synthesis of monodisperse poly(amidoamine) segments (PAAs). By using cystamine as diamine building block in the sequential assembly of dicarboxylic acids, diamines and amino acids, sequence-defined PAA segments with precisely positioned disulfide functionalities could be accessed. The clean incorporation and the selective cleavage of the disulfide moiety in the PAA-main chain were proven by a model system. This consisted of a small PAA-segment covalently attached to the solid-support via a single disulfide linkage. The application of DTT as reducing agent leads to the release of the monodisperse PAA segment as was proven by mass spectrometry analysis.

Polymeric drug carriers, exhibiting a programmed decomposition via reductive triggers, offer some potential advantages for controlled drug delivery. To exemplify this, a poly(ethylene oxide-*block*-amidoamine) (PEO-*block*-PAA) copolymer was synthesized via solid-phase supported synthesis. By positioning a single disulfide linkage between the PAA-segment and the PEO-block a polymeric carrier for gene delivery was accessed. The applicability and the advanced function of the carrier were demonstrated by preparing well-defined polymer DNA complexes (polyplexes). These were analyzed using AFM, light scattering, and gel electrophoresis experiments. A distinct change of the polyplex properties was evident by comparing the untreated polyplexes and the polyplexes after reductive treatment with DTT. The programmed disassembly of the carrier polymer was shown to result in a defined change in the polyplex structure. The reductive removal of the sterically stabilizing PEO-moieties results in a compaction of the polyplex upon development of a positive net charge, while preserving the colloidal stability of the system. A comparable disassembly of the DNA-carriers might occur in the reductive environment of the endosomes, too. It remains to be shown that the intracellular generation of polyplexes with higher surface charge and more compact structure indeed promotes endosomal escape and enhances nucleus localization.

A programmable disassembly of polymeric carriers would be of interest to address other important issues in polymer facilitated drug delivery such as controlled release of pharmacologically active peptide segments or controlled biofade of the polymeric carriers. Moreover, the precise disassembly of the polymeric carrier might also contribute to the fundamental understanding of the mechanisms of polymeric drug delivery, because biological properties can more closely be attributed to polymeric structures and functions. These, however, are subjects of ongoing in vitro cell culture and transfection experiments.

Acknowledgment. Katharina Ostwald, Jessica Brandt, Reinhard Sigel, Birgit Schonert, Anne Heilig, Heike Stephanowitz, Eberhard Krause, Heidi Zastrow, Olaf Niemeyer, Margit Barth, Birgit Erhard, and Erich C. are thanked for the contributions to this project. Financial support was received from the German Research Foundation through the Emmy Noether Program (BO 1762/2-2), the VW Foundation, and the Max Planck Society.

Supporting Information Available: Text discussing the instrumentation and materials, synthesis procedures, and characterization of the polymer carriers, figures showing the MALDI−TOF spectra of **II** and **IVa**, and text giving detailed preparation protocols and characterization of the polyplexes. This material is available free of charge via the Internet at http://pubs.acs.org.

References and Notes

(1) Wagner, E.; Kloeckner, J. *Adv. Polym. Sci.* **2006**, *192*, 135−173.
(2) Ferruti, P.; Marchisio, M. A.; Duncan, R. *Macromol. Rapid Commun.* **2002**, *23*, 332−355.
(3) Ferruti, P.; Manzoni, S.; Richardson, S. C. W.; Duncan, R.; Pattrick, N. G.; Mendichi, R.; Casolaro, M. *Macromolecules* **2000**, *33*, 7793−7800.
(4) Duncan, R. *Nat. Rev. Drug Discov.* **2003**, *2*, 347−360.
(5) Richardson, S.; Ferruti, P.; Duncan, R. *J. Drug Target.* **1999**, *6*, 391−404.
(6) Vuillaume, P. Y.; Brunelle, M.; Van Calsteren, M.-R.; Laurent-Lewandowski, S.; Begin, A.; Lewandowski, R.; Talbot, B. G.; ElAzhary, Y. *Biomacromolecules* **2005**, *6*, 1769−1781.
(7) Lavignac, N.; Lazenby, M.; Foka, P.; Malgesini, B.; Verpilio, I.; Ferruti, P.; Duncan, R. *Macromol. Biosci.* **2004**, *4*, 922−929.
(8) Reineke, T. M.; Liu, Y.; Wenning, L.; Lynch, M. *J. Am. Chem. Soc.* **2004**, *126*, 7422−7423.
(9) Ferruti, P.; Franchini, J. *J. Bioact. Compat. Polym.* **2004**, *19*, 221−236.
(10) Hartmann, L.; Krause, E.; Antonietti, M.; Börner, H. G. *Biomacromolecules* **2006**, *7*, 1239−1244.
(11) Rapp, W. *Combinatorial Peptide and Nonpeptide Libraries*; Jung, G., Ed.; VCH: Weinheim, Germany, New York, and Basel, Swizerland, 1996.
(12) Jain, R.; Standley, S. M.; Fréchet, J. M. J. *Macromolecules* **2007**, *40*, 452−457.
(13) Modi, S.; Jain, J. P.; Domb, A. J.; Kumar, N. *Eur. J. Pharmacol. Biopharm.* **2006**, *64*, 277−286.
(14) Jones, D. P.; Carlson, J. L.; Mody, V. C., Jr.; Cai, J.; Lynn, M. G.; Sternberg, P., Jr. *Free Radical Biol. Med.* **2000**, *28*, 625−635.
(15) Emilitri, E.; Ranucci, E.; Ferruti, P. *J. Polym. Sci., Polym. Chem.* **2005**, *43*, 1404−1416.
(16) Lee, Y.; Koo, H.; Jin, G.; Mo, H.; Cho, M. Y.; Park, J.-Y.; Choi, J. S.; Park, J. S. *Biomacromolecules* **2005**, *6*, 24−26.
(17) Lee, Y.; Mo, H.; Koo, H.; Park, J.-Y.; Cho, M. Y.; Jin, G.; Park, J.-S. *Bioconj. Chem.* **2007**, *18*, 13−18.
(18) Akhtar, S. *Gene Ther.* **2006**; *13*; 739−740.
(19) Rejman, J.; Bragonzi, A.; Conese, M. *Mol. Ther.* **2005**, *12*, 468−474.
(20) Griffiths, P. C.; Paul, A.; Khayat, Z.; Wan, K.-W.; King, S. M.; Grillo, I.; Schweins, R.; Ferruti, P.; Franchini, J.; Duncan, R. *Biomacromolecules* **2004**, *5*, 1422−1427.
(21) Bae, Y.; Nishiyama, N.; Kataoka, K. *Bioconjugate Chem.*, in press
(22) Ritter, W.; Plank, C.; Lausier, J.; Rudolph, C.; Zink, D.; Reinhardt, D.; Rosenecker, J. *Mol. Med.* **2003**, *81*, 708−717.
(23) Henry, S. M.; El-Sayed, M. E. H.; Pirie, C. M.; Hoffman, A. S.; Stayton, P. S. *Biomacromolecules* **2006**, *7*, 2407−2414.
(24) Chan, W. C.; White, P. D. *Fmoc Solid Phase Peptide Synthesis*; Oxford University Press: Oxford, U.K., 2000.
(25) Persson, D.; Thoren, P. E. G.; Lincoln, P.; Norden, B. *Biochemistry* **2004**, *43*, 11045−11055.
(26) Geneste, H.; Hesse, M. *Chem. Unserer Zeit* **1998**, *4*, 206−218.
(27) Vijayanathan, V.; Thomas, T.; Antony, T.; Shirahata, A.; Thomas. T. J. *Nucl. Acid Res.* **2004**, *32*, 127−134.

MA071427U